Effect of 5-Aminolevulinic Acid-Mediated Photodynamic Therapy on MCF-7 and MCF-7/ADR Cells

Tsuimin Tsai, PhD,[1] Ruey-Long Hong, MD, PhD,[2] Jui-Chang Tsai, MD, PhD,[3,5] Pei-Jen Lou, MD, PhD,[4] I-Fang Ling, BS,[5] and Chin-Tin Chen, PhD[5,6]*

[1]*Graduate Institute of Biomedical Materials, Taipei Medical University, Taipei 110, Taiwan*
[2]*Department of Oncology, National Taiwan University Hospital, Taipei 100, Taiwan*
[3]*Department of Surgery (Neurosurgery), National Taiwan University Hospital, Taipei 100, Taiwan*
[4]*Department of Otolaryngology, National Taiwan University Hospital, Taipei 100, Taiwan*
[5]*Center for Optoelectronic Biomedicine, College of Medicine, National Taiwan University; Taipei 100, Taiwan*
[6]*Graduate Institute of Oral Biology, College of Medicine, National Taiwan University; Taipei 100, Taiwan*

Background and Objectives: Photodynamic therapy (PDT) has been proposed as an alternative approach in overcoming multidrug resistance (MDR) phenotype. To verify whether 5-aminolevulinic acid (ALA)-mediated PDT is effective in MDR cells, we studied the protoporphyrin IX (PpIX) content, intracellular localization, and phototoxicity in human breast cancer cells MCF-7 and derived MDR subline, MCF-7/ADR.

Study Design/Materials and Methods: The fluorescence kinetics of ALA-induced PpIX was evaluated by spectrofluorometer. The phototoxicity of MCF-7 and MCF-7/ADR cells was determined by tetrazolium (MTT) assays and clonogenic assay. Furthermore, Annexin V and propidium iodide (PI) binding assays were performed to analyze the characteristics of cell death after ALA–PDT.

Results: MCF-7/ADR accumulated a lower level of PpIX as compared to parental MCF-7 cells. Significant phototoxicity was observed in MCF-7 and increased in a fluence-dependent manner with LD_{50} around 8 J/cm^2. Compared to its parental counterpart, MCF-7/ADR cells were less sensitive to ALA photodynamic treatment and PDT-induced cytotoxicity did not increase in a dose responsive manner as the concentration of ALA increased or the fluence of light increased. ALA–PDT was less effective for MCF-7/ADR cells than MCF-7 cells even under the condition when these two cell lines contained the similar amounts of PpIX.

Conclusions: These results indicate that, except for the MDR related characteristics, MCF-7/ADR cells might possess intrinsic mechanisms that render them less sensitive to ALA–PDT induced phototoxicity. Lasers Surg. Med. 34:62–72, 2004. © 2004 Wiley-Liss, Inc.

Key words: multidrug resistance; photodynamic therapy; protoporphyrin IX; apoptosis

INTRODUCTION

Photodynamic therapy (PDT) has been developed as a modality for cancer treatment, which is based on the administration of photosensitizers to induce cytotoxicity after light irradiation [1,2]. Compared to normal tissues, tumor tissues have higher uptake or retention of photosensitizers that results in the selective eradication of tumor cells. It has been shown that singlet oxygen and other reactive oxygen species (ROS) are responsible for the PDT-induced cell killing that leads to tumor ablation [1,3]. As the primary oxidant associated with the PDT reaction is singlet oxygen, photosensitization has been found to oxidize cellular macromolecules including lipids, proteins, and nucleic acids that result in cell death [4].

5-aminolevulinic acid (ALA) has been successfully used to diagnose and treat neoplastic tissue [5,6]. ALA itself is not a photosensitizer and serves as the biological precursor in the heme biosynthetic pathway [7]. There are two rate-limiting steps in the heme biosynthesis pathway. The first step is the production of ALA from glycine and succinyl CoA, which is regulated by heme via a negative feedback mechanism. The second one is the conversion of protoporphyrin IX (PpIX, the photosensitizer) to heme. This step is controlled by a rate-limiting enzyme, ferrochelatase (FC), which adds a ferrous iron to PpIX. Exogenous ALA administration short-circuits the first step of porphyrin synthesis and leads to the accumulation of PpIX in the tissue. It has been shown that ALA–PDT induced selective destruction of neoplastic lesions attribute to the aberration of heme biosynthesis, such as the reduction of FC activities, in tumor cells [8,9].

Multidrug resistance (MDR) is one of the main obstacles limiting the efficacy of chemotherapy treatment of tumors.

Contract grant sponsor: National Health Research Institute (NHRI); Contract grant number: GT-EX89E840C; Contract grant sponsor: The National Science Council (NSC), Taiwan; Contract grant number: 90-2314-B-002-257.

*Correspondence to: Dr. Chin-Tin Chen, Center for Optoelectronic Biomedicine, College of Medicine, National Taiwan University, No 1, Jen-Ai Road, Section 1st, Taipei 100, Taiwan.
E-mail: ctchen@ha.mc.ntu.edu.tw

Accepted 14 October 2003
Published online in Wiley InterScience (www.interscience.wiley.com).
DOI 10.1002/lsm.10246

As the basic principle of PDT is different from that of traditional chemotherapy, PDT has been considered an alternative approach for the treatment of neoplastic tissues with MDR phenotype. MDR is associated with the overexpression of certain transmembrane proteins such as P-glycoprotein (P-gp), and MDR-associated proteins (MRP), which are cell surface efflux pumps. These proteins can successively purge a wide spectrum of drugs with varying chemical structures or cellular targets from cells [10]. Some studies showed that PDT is effective for the treatment of MDR cells [11–14]. Meanwhile, several observations also reported the cross-resistance to chemotherapeutic drugs and photosensitizers like porphyrin and benzoporphyrin derivatives [15–17]. The failure of PDT in MDR cells could be due to an impaired accumulation of the sensitizer which is excluded by P-gp efflux protein, or could be due to other mechanisms that are not directly related to the P-gp overexpression [18].

MCF-7 is a human breast adenocarcinoma cell line. MCF-7/ADR, a multidrug resistant subline, has been derived by continuous exposure to adriamycin (ADR) [19]. Overexpression of P-gp was found in MCF-7/ADR and may account for its cross-resistance to some of these drugs. However, cross-resistance to non-MDR and non-MRP substrates such as fluorouracil (5-FU) also exists in these cells [20], which cannot be well explained by MDR mechanisms known currently. In fact, multiple biochemical alternations have been noted in MCF-7/ADR cells. Therefore, MCF-7/ADR as well as MCF-7 cells were ideal candidates to investigate PDT resistance. Although it has been reported that P-gp did not mediate ALA or PpIX efflux in certain tumor cells [13,21,22], whether drug-resistant tumor cells show cross-resistance to ALA–PDT is still not clear [13,22]. The objectives of this study were to investigate the fluorescence kinetics of ALA-derived PpIX, PDT-induced cytotoxicity, and cross-resistance to ALA–PDT in MCF-7 cells and its multidrug resistant subline, MCF-7/ADR cells.

MATERIALS AND METHODS

Cell Culture Condition and ALA Incubation

The MCF-7 wild-type human breast cancer cell line and its derivative ADR-resistant (MCF-7/ADR) subline were kindly provided by Dr. Kenneth H. Cowan (NCI, Bethesda, MD). Stock culture of MCF-7 and MCF-7/ADR cells were grown in Eagle's MEM with non-essential amino acid supplemented with 10% fetal calf serum (FCS). Cell cultures were maintained at 37°C in a humidified atmosphere of 95% air and 5% CO_2. The cells seeded in culture plates or dishes were incubated with 1 mM ALA, which was diluted in serum-free medium and neutralized to pH 7.2 with NaOH immediately before use.

Measurement of Protoporphyrin IX

Exponentially growing MCF-7 and MCF-7/ADR cells were seeded at a density of 2×10^5 cells in 6-cm petri-dish. After incubation with ALA (Sigma) for 3 hours, cells were washed with PBS, brought into a solution containing 1 M perchloric acid ($HClO_4$) in 50% methanol, and scraped with a rubber policemen as described by Gaullier et al. [23]. After 5-minute incubation, cell extracts were centrifuged at 1,800*g* for 10 minutes to remove the cell debris. The fluorescence of extracted PpIX was measured in the Aminco-Bowman series 2 spectrofluorometer (SLM Instruments, Urbana, IL) at an excitation wavelength of 405 nm and an emission wavelength of 610 nm. PpIX concentration was deducted from a standard curve of PpIX (6.25–100 ng/ml). The protein content of the cells was determined by the Pierce Micro BCA protein assay method, and the PpIX content was expressed as nmole/mg protein.

Photodynamic Treatment

For photodynamic treatment, cells were seeded in 96-well plates (~7,500 cells/well) and grown overnight in complete medium. After incubation with 1 mM ALA for 3 hours, cells were exposed to various doses of light. The light source was a diode laser with a 633-nm wavelength emission of red light (CeramOptec GmbH, Germany). After irradiation, cells were incubated with fresh complete medium for another 24 hours until further analysis.

Cell Viability Assay

The PDT-induced phototoxicity of MCF-7 and MCF-7/ADR cells was determined by MTT (3-[4,5-dimethylthiazol-2-yl]-2,5-diphenyl tetrazolium bromide, Sigma) as a substrate. The MTT assay is based on the activity of mitochondria dehydrogenases, which can reduce a water-soluble tetrazolium salt to a purple insoluble formazan product. The amount of MTT formazan product was analyzed spectrophotometrically at the absorbance of 570 nm. Cells exposed to ALA but not light were used as a control. Cell survival (%) = (mean OD value of treated cells/mean OD value of control cells) ×100%. Each individual phototoxic experiment was repeated for three times.

Colony-Formation Assay

For colony-formation assay, 500 cells were seeded into 60-mm culture dishes. The next day, after incubation with ALA for 3 hours, cells were exposed to 8 J/cm^2 of light. After light irradiation, cells were washed and further incubated with the complete medium until further analysis. Cells exposed to ALA but not light were used as a control as described above. After incubation for 10 days, the cells were stained with 0.5% crystal violet in 20% ethanol, and colonies of at least 100 cells were counted. For each experiment, four culture dishes were performed. All experiments were carried out in triplicate. The counted colonies were statistically analyzed by ANOVA test.

PpIX Localization in MCF-7 and MCF-7/ADR Cells

Prior to performing the localization of cellular PpIX, cells were seeded into Chamber Slides (Nunc, IL) and incubated for 24 hours. On the next day, cells were incubated with 1 mM ALA for 3 hours. For the last 20 minutes of incubation, cells were stained with 400 nM of MitoTracker® Green (MTG, a well-established fluorescent mitochondria probe, Molecular probe). Cellular PpIX and MTG fluores-

cence were visualized under confocal spectral microscope (Leica, model TCS SP2). The excitation source was a 488 nm argon-ion laser. Fluorescence images of PpIX and MTG were recorded through the control of a monochromator under the condition of 610 ± 20 nm for PpIX and 530 ± 20 nm for MTG. All experiments were performed under ambient light.

Analysis of Mitochondrial Membrane Potential

Prior to examining the mitochondrial membrane potential, cells were seeded into Chamber Slides and incubated for 24 hours. On the next day, cells were incubated with 1 mM ALA for 3 hours. For the last 20 minutes of incubation, cells were stained with 400 nM of MitoTracker® Green or 10 μg/ml of 5,5′,6,6′-tetrachloro-1,1′,3,3′-tetraethylbenzimida-zolylcarbocyanine iodide (JC-1; Molecular Probes) for the examination of mitochondrial structure or mitochondrial membrane potential, respectively. JC-1 is generally accepted as an indicator of mitochondrial membrane potential because it accumulates in mitochondrial as multimeres, depending on the potential across the inner mitochondrial membrane. After light irradiation, cellular images of JC-1 multimeres or MTG fluorescence were visualized under confocal spectral microscope (Leica, model TCS SP2). The fluorescence photographs of JC-1 were recorded upon excitation by a 543 nm He–Ne laser and measured the emission at 590 ± 20 nm. The fluorescence photographs of MTG were recorded upon excitation by a 488 nm argon ion laser and measured the emission at 530 ± 20 nm. All experiments were performed under ambient light.

Apoptosis Analysis

MCF-7 and MCF-7/ADR cells were seeded into Chamber Slides and incubated for 24 hours prior to the study. On the next day, after incubation with ALA for 3 hours, cells were exposed to different doses of light. After ALA–PDT, cells were returned to the complete medium. To examine the apoptotic cells, cells were stained with a mixture of Hoechst 33342 and propidium iodide (PI, Sigma) or Annexin V-FITC [fluorescein isothiocyanate] apoptosis direction kit. Annexin V staining was performed according to the manufacturer's protocol (MBL, Watertown, MA). Staining of the cells with Annexin V-FITC and PI (Sigma) was used to further distinguish between cells undergoing apoptosis (PI negative) and those that were necrotic death (PI positive). After staining, slides were mounted and sealed with nail makeup. Images were obtained with an Olympus inverted fluorescence microscope coupled to a Kodak digital camera.

Statistical Analysis

All experiments were repeated at least three times with 4–6 parallel measurements in different wells or dishes. Resulting values are expressed as the relative number of cells per well or dish compared to the control groups. Results were averaged for experiments performed under similar conditions and expressed as the mean ± SD. The statistical significance of differences in the results was analyzed for statistical significance using unpaired Student's t-test or ANOVA test. A value of $P < 0.05$ was accepted as statistically significant.

RESULTS

Accumulation of ALA Derived PpIX in MCF-7 and MCF/ADR Cells

MCF-7 and MCF-7/ADR cells were incubated with various concentrations of ALA, and PpIX fluorescence was determined at the end of a 3-hour incubation time, which was found to be the maximal accumulation of PpIX. As shown in Figure 1A, accumulation of PpIX in both cell lines was statistically different; PpIX accumulation was

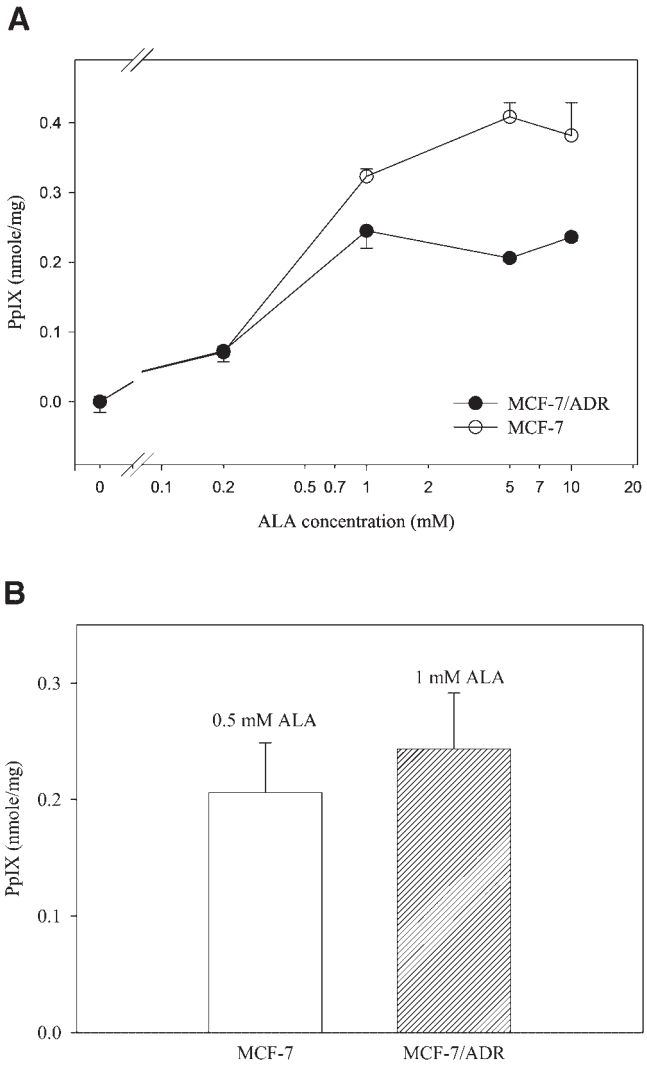

Fig. 1. **A**: Intracellular accumulation of PpIX in MCF-7 and MCF-7/ADR cells. Each point represented the mean value obtained from five independent experiments. (○) MCF-7; (●) MCF-7/ADR. **B**: PpIX accumulation in MCF-7 cells (open bar) under 0.5 mM ALA incubation, MCF-7/ADR cells (hatched bar) under 1 mM ALA incubation. Columns, mean (n = 5); bars, SEM.

lower in MCF-7/ADR cells than in parental MCF-7 cells. Although accumulation of PpIX in both cell lines increased as a function of ALA concentrations, the plateau level of PpIX was at 5 and 1 mM of ALA in MCF-7 and MCF-7/ADR cells, respectively. The data in Figure 1B further indicate that, under 0.5 mM of ALA incubation, MCF-7 cells accumulated no significant difference of PpIX content as 1 mM ALA did in MCF-7/ADR cells.

Photodynamic Effects on MCF-7 and MCF-7/ADR Cells

To analyze the PDT-induced cytotoxicity, MCF-7 and MCF-7/ADR cells were incubated with 1 mM ALA and irradiated with various doses of light. Cellular viabilities were estimated by MTT assay at 24 hour after light irradiation. As shown in Figure 2A, significant phototoxicity

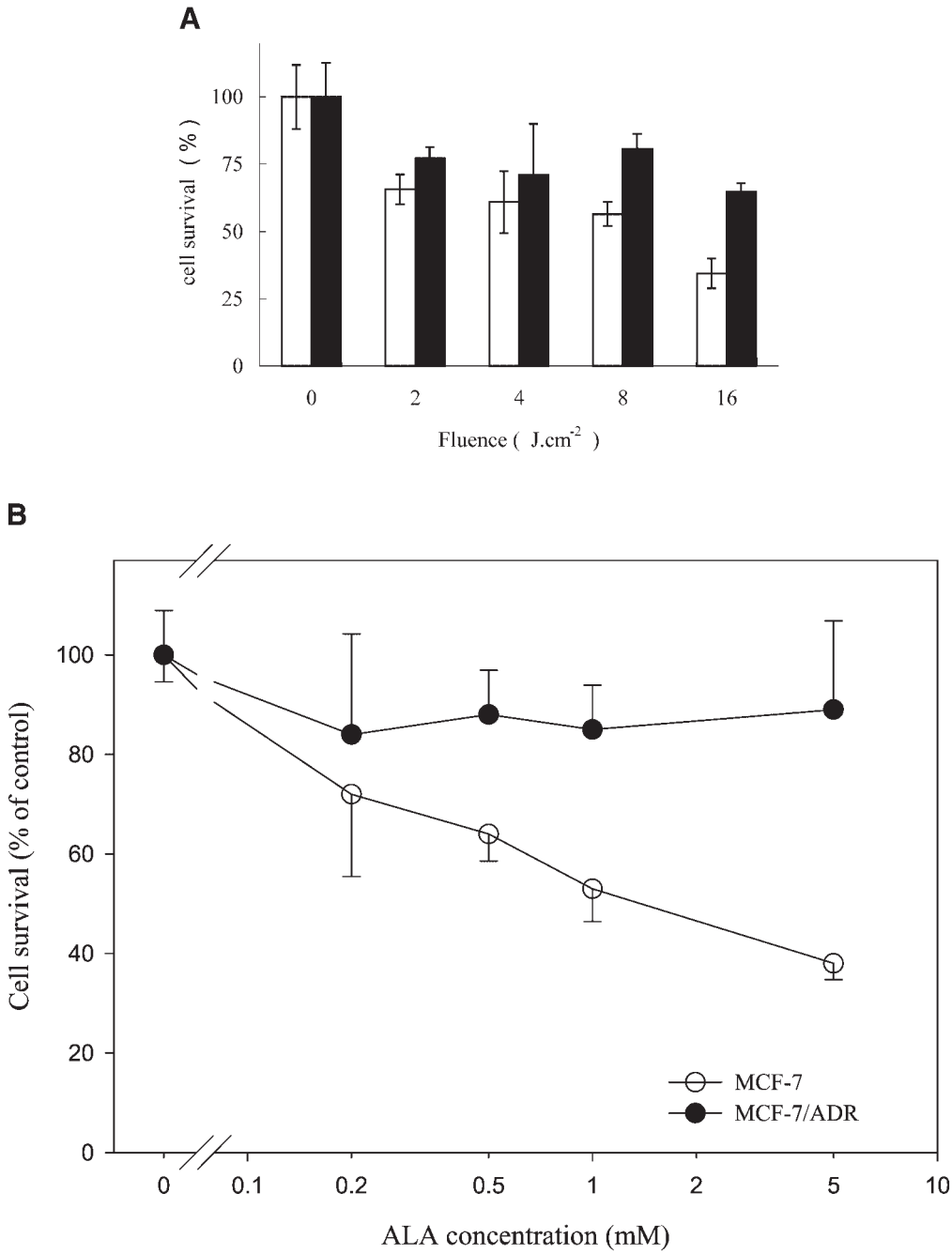

Fig. 2. ALA–PDT induced cytotoxicity. **A**: MCF-7 (□) and MCF-7/ADR (■) cells were incubated with 1 mM ALA and exposed to light irradiation at different light fluence. **B**: MCF-7 (○) and MCF-7/ADR (●) cells were incubated with different concentrations of ALA and exposed to 8 J/cm^2 of light. Cell viability was assessed by MTT assay 24 hours after light irradiation. Data are mean ± SEM obtained from three independent experiments.

was observed in MCF-7 and increased in a fluence-dependent manner with LD_{50} around 8 J/cm^2. Importantly, without ALA incubation, less than 5% of the cells died under the light dose of 8 J /cm^2. Compared to its parental counterpart, MCF-7/ADR cells were less sensitive to ALA photodynamic treatment, and PDT-induced cytotoxicity did not increase in a fluence-dependent manner. Similar results were also observed in the cells treated with various concentrations of ALA. As shown in Figure 2B, MCF-7 cells were more sensitive to ALA–PDT as compared to MCF-7/ADR cells. The survival rate of MCF-7 cells, but not MCF-7/ADR cells, was significantly decreased as the ALA concentration increased.

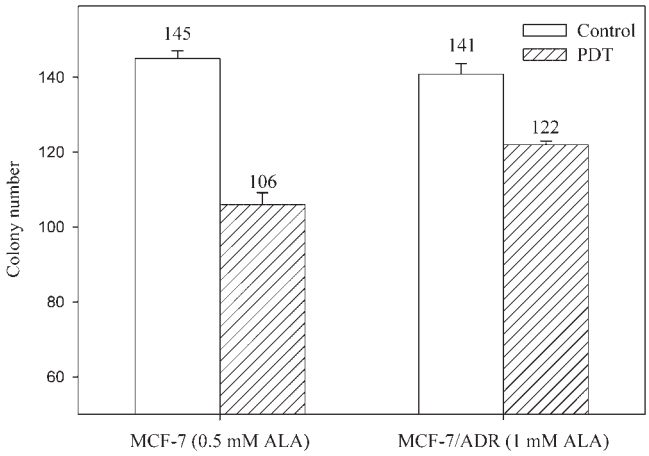

Fig. 3. Cell viability measurement via clonogenic assay. Values shown represent the total number of colonies calculated from control and PDT-treated plates and represent the average values obtained from four separate plates. Compared to non-PDT-treated cells, the average cell viability of MCF-7 and MCF-7/ADR were 73.1 and 86.7%, respectively.

Differential PDT-Induced Phototoxicity Between MCF-7 and MCF-7/ADR Cells was not Due to the Different PpIX Content

As indicated above, under the same ALA incubation condition, the accumulation of PpIX in MCF-7/ADR cells is lower than in parental MCF-7 cells. In this regard, it is reasonable to assume that lower PpIX might cause the lower cytotoxicity in MCF-7/ADR cells after light irradiation. As shown in Figure 1B, under a concentration of 0.5 mM ALA, the accumulated PpIX level in MCF-7 is not significantly different from that of 1 mM ALA in MCF-7/ADR cells (0.21 ± 0.04 and 0.24 ± 0.05 for MCF-7 and MCF-7/ADR, respectively; $P > 0.05$). However, even at the similar level of PpIX, the cytotoxicity of MCF-7 is 20% higher than that of MCF-7/ADR under the light dose of 8 J/cm^2 (Fig. 2B). These results suggest that the differential ALA–PDT cytotoxicity between MCF-7 and MCF-7/ADR cells was not due to the lower level of PpIX content.

In this study, we used MTT assay to verify the ALA–PDT induced phototoxicity. The method is commonly used in evaluating cells which have lost the activity of mitochondria dehydrogenases after treatment. The last step of ALA conversion to PpIX is localized at the mitochondria, which might cause differences in timing and degree of functional impairment after light irradiation. In addition, the rates of cell proliferation and cell death between MCF-7 and MCF-7/ADR cells are different after ALA–PDT. To avoid misinterpretation of the overall death of both cell lines using MTT assay, the clonogenic assay was performed to assess the proliferation ability after ALA–PDT. As shown in Figure 3, the clonogenic survival rate of MCF-7 and MCF-7/ADR is 73.1 and 86.7%, respectively. There is a statistically significant difference ($P \leq 0.031$ by two-way ANOVA). This result clearly showed that MCF-7 cells were more responsive to ALA–PDT, which is consistent with our observation in MTT assay (Fig. 2B). These findings indicated that the different PDT response between MCF-7 and MCF-7/ADR cells was not due to the altered content of PpIX.

ALA–PDT Induced Mitochondrial Photodamages

Since the intracellular photosensitizer distribution plays a decisive role in photodynamic efficacy [24,25], the differential phototoxicity between MCF-7 and MCF-7/ADR cells might be due to the different distribution patterns of PpIX. To examine the localization of PpIX in MCF-7 and MCF-7/ADR cells, fluorescence images of PpIX were examined under confocal fluorescence microscope. As the conversion of ALA to PpIX is mainly at mitochondria, MitoTracker® Green, a well-established fluorescent mitochondria probe, was used to localize the mitochondria. After 3-hour of ALA incubation, PpIX is mainly localized at mitochondria as shown by the significant overlapped images in MCF-7 and MCF-7/ADR cells (Fig. 4). These results suggest that the subcellular distribution of PpIX in MCF-7 and MCF-7/ADR cells is mainly localized at mitochondria.

Due to the short diffusion distance of singlet oxygen, the sites of direct photodamage could be correlated to the sites of photosensitizer location [26]. In the present study, we demonstrated that most PpIX is mainly localized at mitochondria, suggesting that mitochondrial photodamages could be induced after light irradiation. As shown in Figure 5A, ALA–PDT induced an immediate collapse of mitochondrial membrane potential as detected by JC-1 dye, a mitochondrial membrane potential sensitive dye, in MCF-7 and MCF-7/ADR cells. However, the labeling pattern of MitoTracker® Green (MTG) dye, which is independent of mitochondrial membrane potential, in the stained cells remained unchanged after ALA–PDT (Fig. 5B), suggesting that the mitochondrial organelle structure in the ALA–PDT treated cells was reserved.

Characterization of ALA–PDT-Induced Cell Death

As shown above, ALA–PDT causes mitochondrial photodamages, indicating that apoptosis could be induced

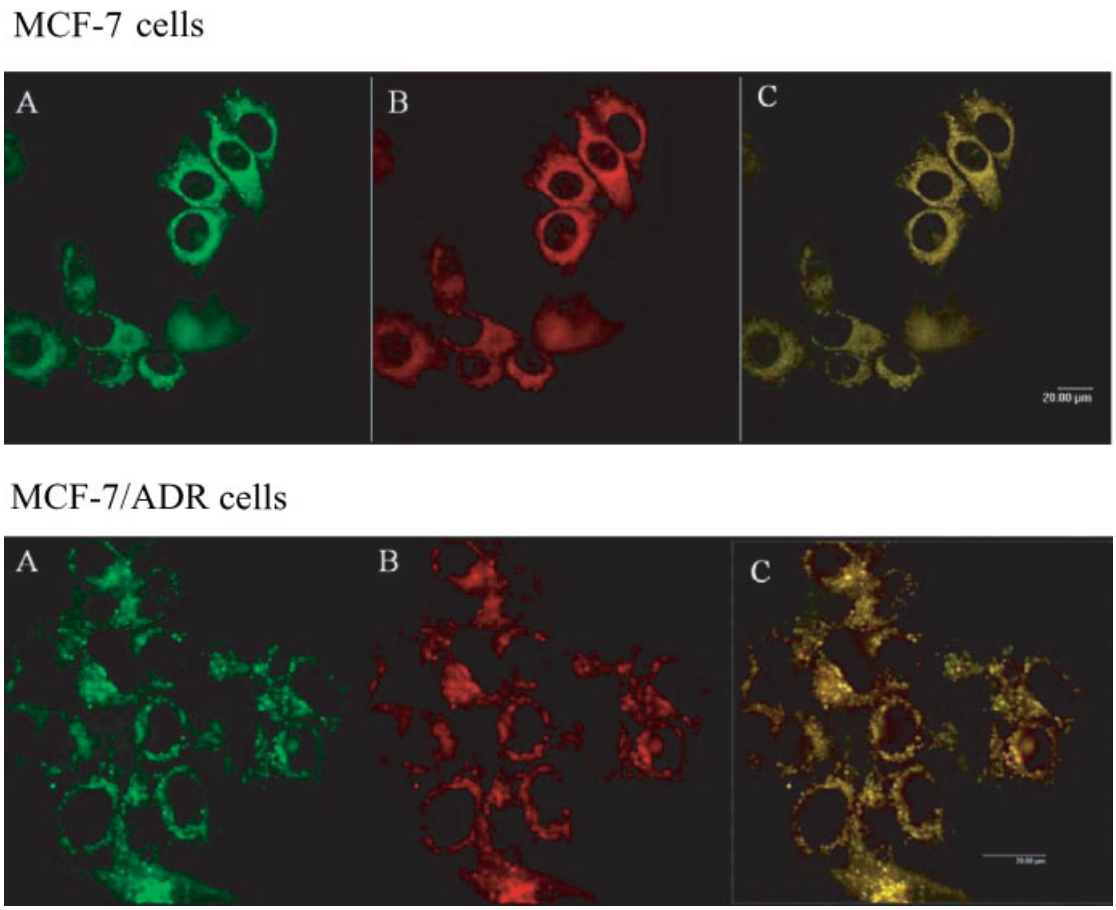

Fig. 4. Confocal microscopic analysis of cellular (**A**) PpIX and (**B**) MitoTracker® Green (MTG) fluorescence in MCF-7 cells incubated with 1 mM ALA for 3 hours, and then with MTG for 10 minutes. **C**: Co-localization for mitochondria. Fluorescence photographs were taken through the control of a monochromator under the condition of 610 ± 20 nm for PpIX and 530 ± 30 nm for MTG.

[27,28]. Apoptotic cell death is defined by the occurrence of a stereotype phenotype including cell shrinkage, chromatin condensation, and nuclear fragmentation. To verify the mode of cell death, ALA–PDT treated MCF-7 cells were stained with the DNA intercalating dye (Hoechst 33342) to assess the apoptotic characteristic of nuclear condensation. On the other hand, the staining of nuclei with PI was performed to detect the plasma membrane damage, which is known to be a marker of necrosis. As shown in the upper panel of Figure 6A, MCF-7 cells underwent nuclear condensation as observed by Hoechst 33342 staining, but not the staining of nuclei with PI 4 hour post ALA–PDT (8 J/cm^2). However, under the light dose of 16 J/cm^2, nuclear condensation of Hoechst 33342 staining positive cells also stained positively for PI, suggesting that MCF-7 might also undergo necrosis (lower panel of Fig. 6A). Annexin V has been used to detect the externalization of phosphatidylserine (PS) occurred at an early stage of apoptosis. When the necrotic cell death occurred, the cytoplasmic membrane permeability is increased, and both Annexin V and PI can enter the cell and bind to intracellular PS and DNA, respectively. Therefore, we performed a fluorescein isothiocyanate (FITC)-conjugated annexin V binding assay to confirm that ALA–PDT induced apoptosis in MCF-7 cells. As shown in the left panel of Figure 6B, in the outer cell membrane of PDT-treated MCF-7 cells show a clear Annexin V staining with green fluorescence 4 hour after light irradiation (8 J/cm^2). The PI negative staining further indicates that the cell membrane remains intact in most MCF-7 cells (right panel, Fig. 6B). In contrast, MCF-7/ADR did not show clear chromosome condensation or PI positive staining 4 hour post ALA–PDT under the light dose of 8 or 16 J/cm^2 (Fig. 6C).

DISCUSSIONS

In this report, we showed that 1 mM of ALA treatment caused less accumulation of PpIX and phototoxicity induced by light irradiation in MCF-7/ADR cells than in parental MCF-7 cells. However, the differential phototoxicity could not be attributed to the different PpIX contents in the parental and ADR resistant cells. As shown in

Figure 1B, treatment of MCF-7 cells with 0.5 mM ALA and MCF-7/ADR cells with 1 mM ALA caused no significant difference in PpIX accumulation. However, MTT and clonogenic assays showed that the cell viability of MCF-7 is significantly lower than that of MCF-7/ADR under the light dose of 8 J/cm^2 (Figs. 2B and 3). Furthermore, the survival rate of MCF-7/ADR cells was not significantly decreased as the ALA concentration or fluence increased (Fig. 2). These results indicate that the multidrug resistant MCF-7/ADR cells have partial resistance to ALA–PDT, which could not be simply explained by the classical MDR characteristics.

It has been reported that the differential phototoxicity between resistant and parental cells might be related to the different intracellular localization of PpIX [24,25]. As shown in Figure 4, we found that the intracellular localization of PpIX is no difference between MCF-7 and MCF-7/ADR cells. In addition, mitochondrial photodamages were found in both cell lines as shown by the collapsed membrane potential with reserved organelle structure following ALA–PDT treatment (Fig. 5). These results indicate that the differential phototoxicity between these two cell lines could not be attributed to the different subcellular targets of PpIX.

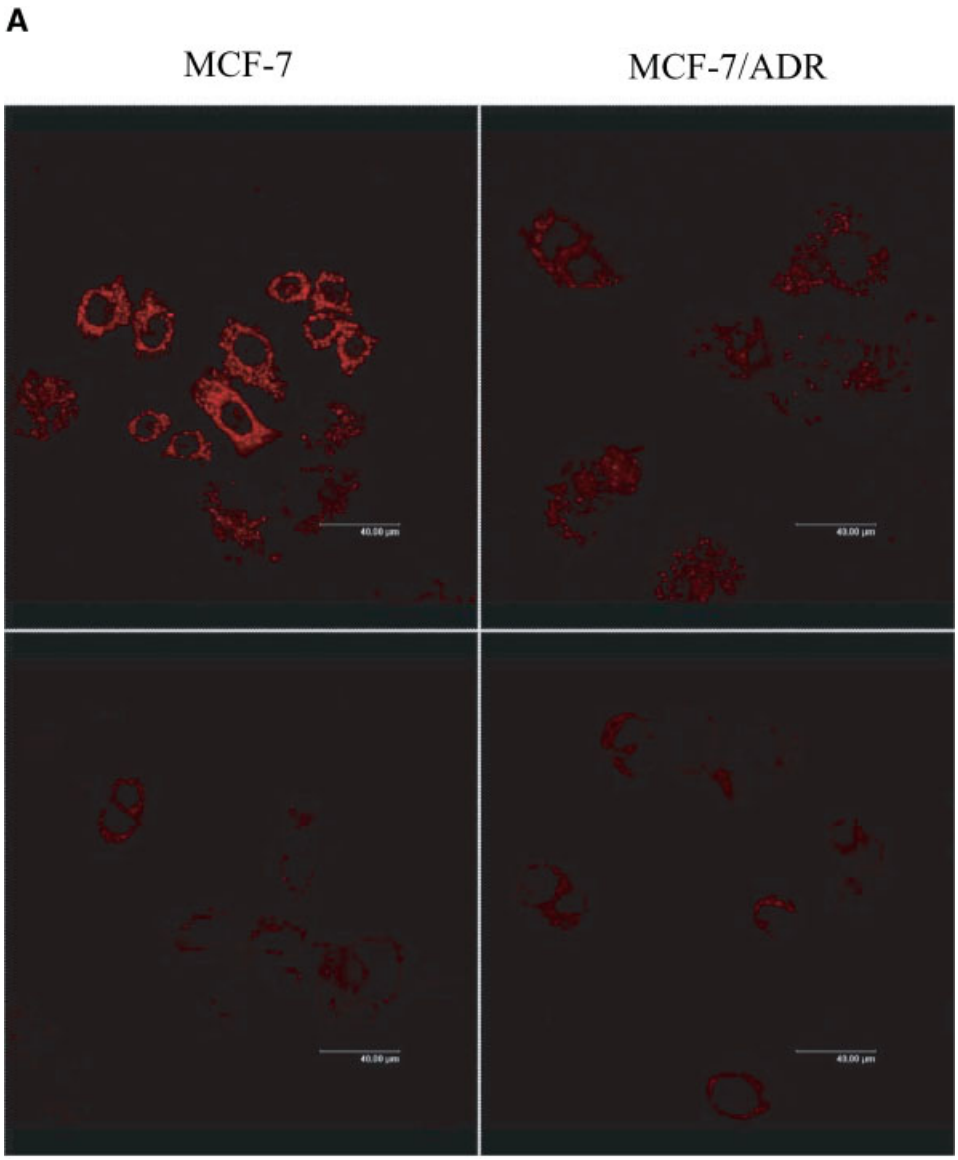

Fig. 5. Mitochondrial fluorescence pattern in MCF-7 and MCF-7/ADR cells after ALA–PDT. **A**: JC-1 labeling cells treated with light only (**upper panel**) or ALA–PDT (**lower panel**) 30 minutes post light irradiation under the light dose of 8 J/cm^2 (LD_{50}); (**B**) MTG labeling cells treated with light only (**upper panel**) or ALA–PDT (**lower panel**) 30 minutes post light irradiation under the light dose of 8 J/cm^2 (LD_{50}).

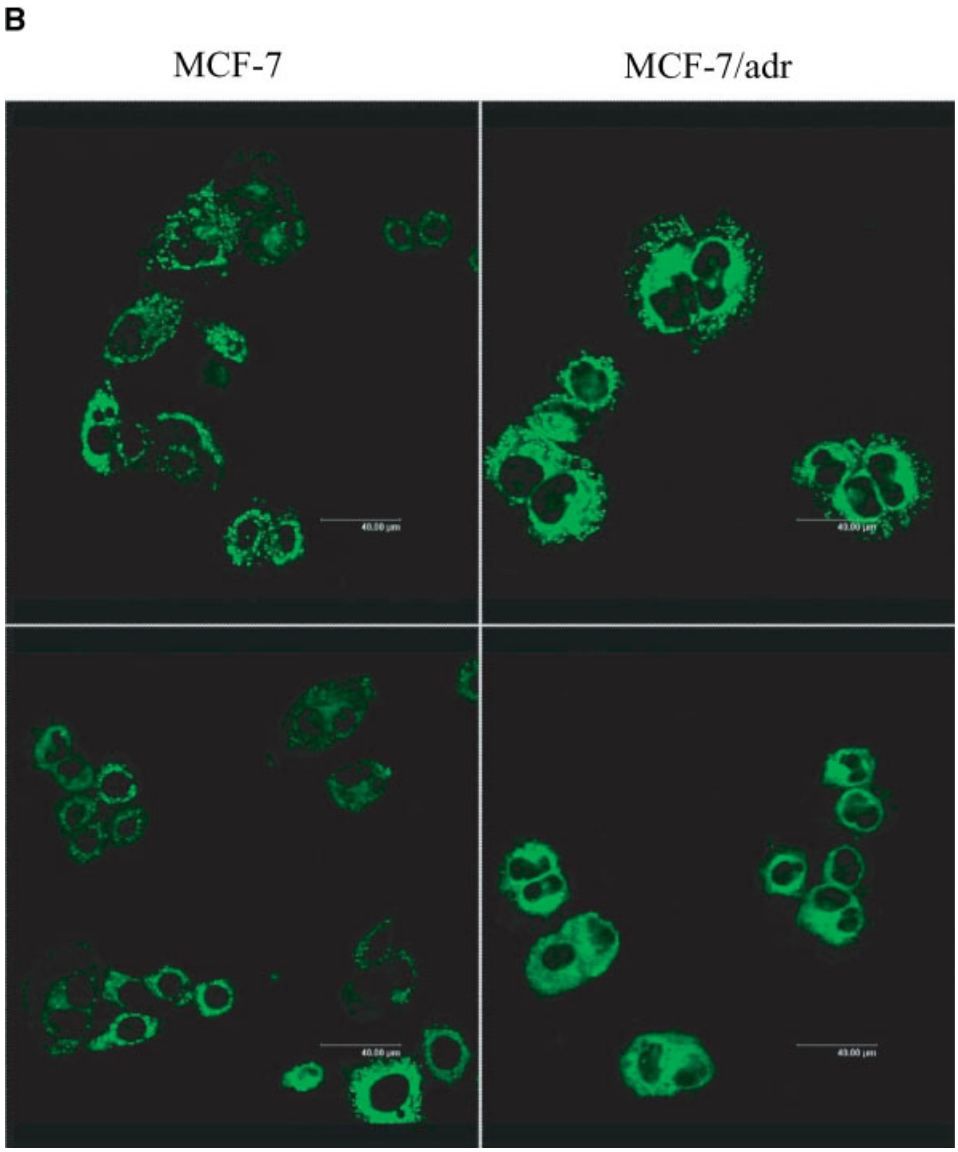

Fig. 5. (*Continued*)

Cellular photodamages associated with PDT have been ascribed to cytoplasmic membrane, mitochondria, lysosome, endoplasmic reticulum (ER), and Golgi depending on the photosensitizers [29]. The different subcellular localization of photosensitizer might induce different cellular effects by either rescue response or by undergoing cell death. In a current study, we employed ALA–PDT to induce mitochondrial photodamages, which initiate a greater phototoxicity in MCF-7 cells as compared to MCF-7/ADR cells. It is interesting to compare our data with the studies performed by Bezdetnaya's group [14]. They demonstrated that mTHPC-based PDT was more effective in killing MCF-7/DXR cells, which express the MDR phenotype. In fact, our unpublished results also indicated that the survival rate of MCF-7/ADR cells was 30% lower than that of MCF-7 via clonogenic assay using mTHPC as a photosensitizer (data not shown). One possible explanation for this contradiction might be attributed to the specific localization of PpIX and mTHPC. Bezdetnaya's PDT study in MCF-7/DXR cells demonstrated that the observed mTHPC localization was in the intracytoplasmic vesicles in which lysosomes are resembled both in location and size [14]. In fact, a recent report published by the same group further indicated that ER and Golgi are the preferential sites of mTHPC in MCF-7 cells [30]. Based on these, it is obvious that mitochondria were not the photodamaged target by mTHPC-based PDT due to the short lifetime and diffusible distance of the PDT mediator, singlet oxygen. In contrast, under our experimental condition, mitochondria are the main photodamged targets of PpIX, which results in

significant toxicity in MCF-7, but not MCF-7/ADR cells, after ALA–PDT treatment. Therefore, these results indicate that the differential PDT-induced cytotoxicity mediated by ALA and mTHPC might be related to the targeted photosensitizer localization in MCF-7 and derived drug resistant cells.

Bcl-2, a protein located outside the mitochondrial membrane, has profound influences on the sensitivity of cellular apoptosis. The protective role of Bcl-2 in PDT-induced cell death has been shown in many reports [31,32]. As shown in Figure 6, ALA–PDT induced the occurrence of apoptosis in MCF-7 cells but not MCF-7/ADR cells. Accordingly, it is reasonable to assume that alterations of Bcl-2 might be involved in the partial resistance of MCF-7/ADR to ALA–PDT. However, Western blot analysis showed that there is no significant difference on the Bcl-2 levels between MCF-7 and MCF-7/ADR cells (data not shown), suggesting that the partial resistance in MCF-7/ADR might not be related to the abnormal protein level of Bcl-2.

In summary, this study clearly indicates that the differential phototoxicity between MCF-7 and MCF-7/ADR cells was not due to the different levels of PpIX or its targets. Substantial ultrastructural changes and altered membrane potential of mitochondria has been observed in PDT and cisplatin cross-resistant cell line [33,34]. As mitochondria are the main photodamaged targets in our

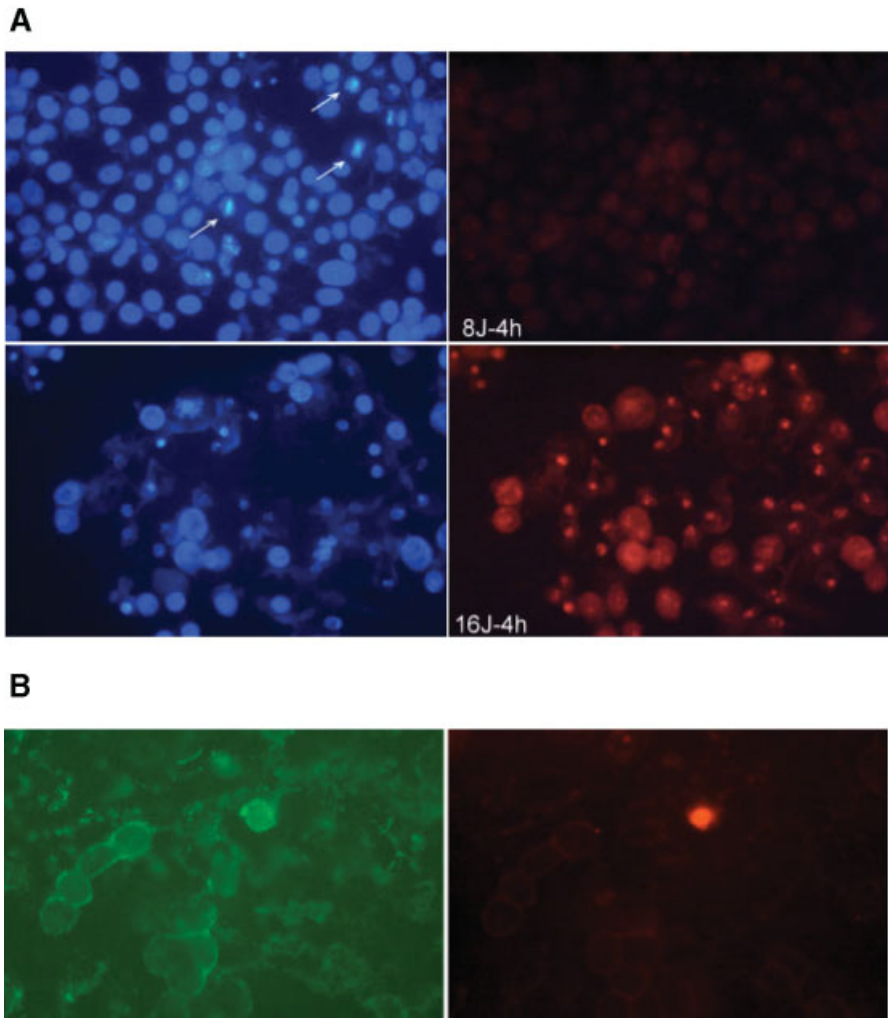

Fig. 6. Fluorescence photographs of MCF-7 and MCF-7/ADR cells treated with ALA–PDT and stained with Hoechst 33342 (blue), PI (red) and annexin V (FITC labeled: green) at indicated time post light irradiation. **A**: MCF-7 cells stained with Hoechst 33342 (**left panel**) and PI (**right panel**) under the light dose of 8 J/cm^2 (**upper panel**) or 16 J/cm^2 (**lower panel**). Note positive for Hoechst 33342 staining (arrows) and negative PI nuclei staining indicate apoptotic cells under the light dose of 8 J/cm^2. **B**: MCF-7 cells stained with Annexin V (green fluorescence in the outer cell membrane, **left panel**) represent apoptosis, while cells without PI-stained nuclei (**right panel**) under the light dose of 8 J/cm^2. **C**: MCF-7/ADR cells stained with Hoechst 33342 (**left panel**) and PI (**right panel**) under the light dose of 8 J/cm^2 (**upper panel**) or 16 J/cm^2 (**lower panel**).

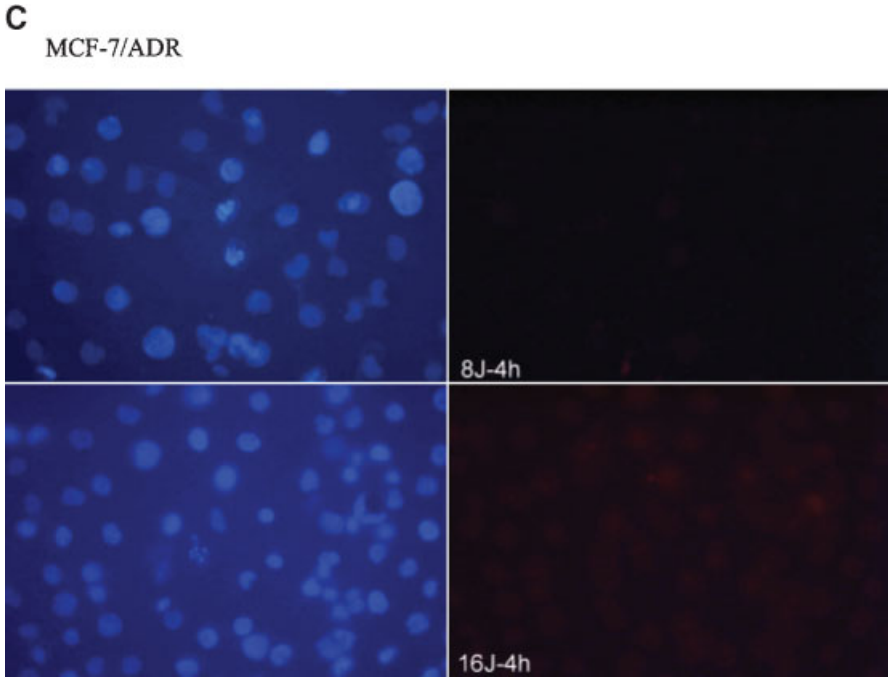

Fig. 6. (*Continued*)

present studies, further studies on the alterations of mitochondrial characteristics and extended biochemical pathways are under investigation.

ACKNOWLEDGMENTS

The authors thank Miss Li-Ting Chien for her assistance with the experiments and Dr. Wen-Sen Lee for several fruitful discussions.

REFERENCES

1. Henderson BW, Dougherty TJ. How does photodynamic therapy work? Photochem Photobiol 1992;55:145–157.
2. Dolmans DEJGJ, Fukumura D, Jain RK. Photodynamic therapy for cancer. Nat Rev Cancer 2003;3:380–387.
3. Gomer CJ, Rucker N, Ferrario A, Wong S. Properties and applications of photodynamic therapy. Radiat Res 1989; 120:1–18.
4. Boyle RW, Dolphin D. Structure and biodistribution relationships of photodynamic sensitizers. Photochem Photobiol 1996;64:469–485.
5. Kennedy J, Pottier RH, Pross DC. Photodynamic therapy with endogenous protoporphyrin IX. Basic principles and present clinical experience. J Photochem Photobiol B Biol 1990;6:143–148.
6. Peng Q, Berg K, Moan J, Kongshaug M, Nesland JM. 5-aminolevulinic acid-based photodynamic therapy: Principles and experimental research. Photochem Photobiol 1997;65: 235–251.
7. Gardner LC, Smith SJ, Cox TM. Biosynthesis of δ-aminolevulinic acid and the regulation of heme formation by immature erythroid cells in man. J Biol Chem 1991;266: 22010–22018.
8. Dailey HA, Smith A. Differential interaction of porphyrins used in photoradiation therapy with ferrochelatase. Biochem J 1984;223:441–445.
9. Gibson SL, Nguyen ML, Havens JJ, Barbarin A, Hilf R. Relationship of δ-minolevulinic acid-induced protoporphyrin IX levels to mitochondrial content in neoplastic cells in vitro. Biochem Biophy Res Commu 1999;265:315–321.
10. Gottesman M, Pastan I. Biochemistry of the multidrug resistance mediated by the multidrug transporter. Ann Rev Biochem 1993;62:385–427.
11. Kessel D, Erickson C. Prophyrin photosensitization of multidrug resistant cell types. Photochem Photobiol 1992;55:397–399.
12. Frazier DL, Barnhill MA, Lu X, Jones E, Niemeyer G, Mishu L, Lothrop CD, Jr. Effect of multidrug-resistant P-glycoprotein gene expression on chloroaluminum tetrasulfonate phthalocyanine concentration. Lasers Surg Med 1993;13: 511–516.
13. Li W, Zhang WJ, Ohnishi K, Yamada I, Ohno R, Hashimoto K. 5-aminolevulinic acid-mediated photodynamic therapy in multidrug resistant leukemia cells. J Photochem Photobiol B Biol 2001;60:79–86.
14. Teiten M-H, Bezdetnaya L, Merlin J-L, Bour-Dill C, Pauly ME, Dicato M, Guillemin F. Effect of meta-tetra(hydroxyphenyl)chlorin (mTHPC)-mediated photodynamic therapy on sensitive and multidrug-resistant human breast cancer cells. J Photochem Photobiol B Biol 2001;62:146–152.
15. Lemoli RM, Igarashi T, Knizewski M, Acaba L, Richter A, Jain A, Mitchell D, Levy J, Gulati SC. Dye-mediated photolysis is capable of eliminating drug-resistant (MDR^+) tumor cells. Blood 1993;1:793–800.
16. Kessel D, Woodburn K, Skalkos D. Impaired accumulation of a cationic photosensitizing agent by a cell line exhibiting multidrug resistance. Photochem Photobiol 1994;60:61–63.
17. Kessel D, Woodburn K. Selective photodynamic inactivation of a multidrug transporter by a cationic photosensitizing agent. Br J Cancer 1995;71:306–310.
18. Moorehead RA, Armstrong SG, Wilson BC, Singh G. Cross-resistance to cisplatin in cells resistant to photofrin-mediated photodynamic therapy. Cancer Res 1994;57:2556–2559.
19. Fairchild CR, Ivy SP, Kao-Shan CS, Whang-Peng J, Roen N, Israel MA, Melera PW, Cowan KH, Goldsmith ME. Isolation of amplified and overexpressed DNA sequences from adriamycin-resistant human breast cancer cells. Can Res 1987;47: 5141–5148.
20. Chu E, Drake JC, Koeller DM, Zinn S, Jamis-Dow CA, Yeh GC, Allegra CJ. Induction of thymidylate synthase associated

with multidrug resistance in human breast and colon cancer cell lines. Mol Pharm 1991;39:136–143.
21. Rossi FM, Campbell DL, Pottier RH, Kennedy JC, Dickson EF. In vitro studies on the potential use of 5-aminolaevulinic acid-mediated photodynamic therapy for gynaecological tumours. Br J Cancer 1996;74:881–887.
22. Datta SN, Allman R, Loh CS, Mason M, Matthews PN. Photodynamic therapy of bladder cancer cell lines. Br J Urol 1997;80:421–426.
23. Gaullier JM, Berg K, Peng Q, Anholt H, Selbo PK, Ma L-W, Moan J. Use of 5-aminolevulinic acid esters to improve photodynamic therapy on cells in culture. Can Res 1997;57: 1481–1486.
24. Liang H, Shin DS, Lee YE, Nguyen DC, Trang TC, Pan AH, Huang SL, Chong DH, Berns MW. Subcellular phototoxicity of 5-aminolevulinic acid (ALA). Lasers Surg Med 1998;22:14–24.
25. Gaullier JM, Geze M, Santus R, Sa e Melo T, Maziere JC, Bazin M, Morliere P, Dubertret L. Subcellular localization and photosensitization by protoporphyrin IX human keratinocytes and fibroblasts cultivated with 5-aminolevulinic acid. Photochem Photobiol 1995;62:114–122.
26. Peng Q, Moan J, Nesland JM. Correlation of subcellular and intratumoral photosensitizer localization with ultrastructural features after photodynamic therapy. Ultrastruct Pathol 1996;20:109–129.
27. Kessel D, Luo Y, Deng Y, Chang CK. The role of subcellular localization in initiation of apoptosis by photodynamic therapy. Photochem Photobiol 1997;65:422–426.
28. Kessel D, Luo Y. Mitochondrial photodamage and PDT-induced apoptosis. J Photochem Photobiol B 1998;42:89–95.
29. Oleinick NL, Evans HH. The photobiology of photodynamic therapy: Cellular targets and mechanisms. Radiat Res 1998; 150:S146–156.
30. Teiten M-H, Bezdentnaya L, Morliere P, Santus R, Guillemin F. Endoplasmic reticulum and Golgi apparatus are the preferential sites of Foscan® localization in tumor cells. Br J Cancer 2003;88:146–152.
31. He J, Agarwall ML, Larkin HE, Friedman LR, Xue LY, Oleinick NL. The induction of partial resistance to photodynamic therapy by the protooncogene bcl-2. Photochem Photobiol 1996;64:845–852.
32. Zhang WG, Ma LP, Wang SW, Zhang ZY, Gao GD. Antisense bcl-2 retrovirus vector increases the sensitivity oh a human gastric adenocarcinoma cell line to photodynamic therapy. Photochem Photobiol 1999;69:582–586.
33. Sharkey SM, Wilson BC, Moorehead R, Singh G. Mitochondrial alterations in photodynamic therapy-resistant cells. Cancer Res 1993;53:4994–4999.
34. Moorehead RA, Armstrong SG, Wilson BC, Singh G. Cross-resistance to cisplatin in cells resistant to photofrin-mediated photodynamic therapy. Cancer Res 1994;54:2556–2559.